Hypergeometric solutions to a three dimensional dissipative oscillator driven by aperiodic forces

(Article begins on next page)

21 February 2025

Hypergeometric solutions to a three dimensional dissipative oscillator driven by aperiodic forces

Alessio Bocci, Giovanni Mingari Scarpello, Daniele Ritelli

Abstract

We model the dynamical behavior of a three dimensional (3-D) dissipative oscillator consisting of a m-block whose vertical fall occurs against a spring and which can also slide horizontally on a rigid truss rotating at an assigned angular speed $\omega(t)$. The bead's z-vertical time law is obvious, whilst its x-motion along the horizontal arm is ruled by a linear differential equation we solve through the Hermite functions and the Kummer [1] confluent Hypergeometric Function (CHF) $_1F_1$. After the rotation $\theta(t)$ has been computed, we know completely the m-motion in a cylindrical frame reference so that some transients have then been analyzed. Finally, further effects as an inclined slide and a contact dry friction have been added to the problem, so that the motion differential equation becomes inhomogeneous: we resort to Lagrange method of variation of constants, helped by a Fourier-Bessel expansion, in order to manage the relevant intractable integrations.

Keywords: Coriolis theorem; Kummer hypergeometric function; Hermite function; Lagrange variation of constants; Fourier-Bessel expansion.

1   Introduction

1.1   Aim of the problem

Almost all types of oscillations have been the subject of intensive research for many years and several methods have been used to find exact/approximate solutions to such dynamical systems. The oscillator hereinafter analyzed, is moving along three directions: its motion (main) ordinary differential equations is linear with variable coefficients. Such a dissipative oscillator undertakes: own weight, constraint reaction, Coriolis force, centrifugal force, elastic forces, viscous resistance and the inertia force due to the angular acceleration $\dot{\omega}$. All the analytical evaluations have been performed without any approximation. After that dry friction has been added, the particular integral of the consequent inhomogeneous equation could only be found by means of variation of constants. Let us introduce the system main features.

A rotating blade is modeled by a rod of length $2L$ on which a mass m is sliding, secured to the hub Ω by a spring of stiffness k_2. The rod is jointed at Ω to a vertical shaft of length H: the heavy block's vertical motion is against a spring of stiffness k_1. Therefore the bead P modeling the m-block, has a 3-D motion[1]: its position is set out by a cylindrical coordinate frame with x, z, θ depending on time. The first two co-ordinates, unknown functions of time, are the object of our inquiry; the third one is decided by $\omega(t)$. Such a model, with an obvious change, will also describe the effects induced by an increasing angular speed ω from a rest up to an absolute maximum.

We put a reference frame (x, y, z) co-mobile with the rod, so that the $x-$motion of the block, which can move on both sides with respect to the hub Ω, is referred to such a non-inertial frame. In such a case, the Coriolis theorem here arises in its complete six terms formulation:

$$\mathbf{a}_r = \mathbf{a}_a - \mathbf{a}_\Omega - \boldsymbol{\omega} \wedge (\boldsymbol{\omega} \wedge \ \boldsymbol{r}) - 2\boldsymbol{\omega} \wedge \boldsymbol{v}_r - \dot{\boldsymbol{\omega}} \wedge \boldsymbol{r}. \tag{1.1}$$

The problems whose closed form solution comes out taking *all the terms* of Coriolis theorem are presumably very few: we cannot cite any one of them.

The CHFs are usually occurring in Mathematical Physics after splitting a linear partial differential equations in more ordinary differential equations. Their use for linear or nonlinear Mechanics problems is not much practiced. We can refer for instance to [3], [4], [5]. On the contrary, much

---

[1]Another paper concerning a rod 3-D problem but involving elliptic functions is [2]

greater is their appearance in quantum mechanics: in [6] we meet CHFs in treatments on the one-dimensional harmonic oscillator and in the isotropic one. Monographic, quite old, but authoritative books are [7] and [8] as well. An extensive more recent introduction to CHFs can be found in [9] which holds a bibliography of 89 entries. In [10], several properties of extended CHFs are studied showing how they are met in statistical distribution theory.
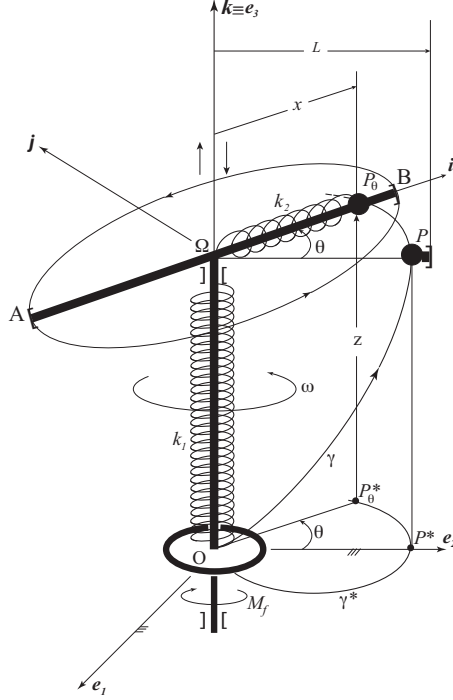
1.2   The mathematical model

Figure 1: A 3-D oscillator and its co-mobile reference frame.

With reference to Figure 1, let the mobile frame be rotating around a fixed one: if $\boldsymbol{k}$ is the unit vector on the vertical direction Ωz, the angular speed will be $\boldsymbol{\omega} = \omega_0(1 - qt)\boldsymbol{k}$ so that the angular acceleration is: $\dot{\boldsymbol{\omega}} = -\omega_0 q \boldsymbol{k}$. The third co-mobile is the Ωy-axis of unit vector $\boldsymbol{j}$ orthogonal to the Ωx one. Multiplying to m, mass of the bead P, by (1.1) we get the forces a co-mobile observer sees acting on the bead. They are:

• the force due to the motion of the mobile reference system with respect to the fixed one: $m\boldsymbol{a}_\Omega = m\ddot{z}\boldsymbol{k}$,

• the "absolute" force given by $m\boldsymbol{a}_a = (-k_2 x - A\dot{x}(t))\boldsymbol{i} + R_y\boldsymbol{j} + (R_z - mg)\boldsymbol{k}$, being the resistance $A\dot{x}(t)$ produced by a viscous damper, with $A > 0$ drag coefficient. Notice that $\boldsymbol{R} = (0, R_y, R_z)$ is the constraint unknown reaction from the rod on the m-bead,

• the centrifugal force: $m\boldsymbol{\omega} \wedge (\boldsymbol{\omega} \wedge \boldsymbol{r}) = -m\omega_0^2(1 - qt)^2 x\boldsymbol{i}$,

• the Coriolis force: $m\boldsymbol{\omega} \wedge \boldsymbol{v}_r = m\omega_0(1 - qt)\dot{x}\boldsymbol{k}$,

• eventually, the inertia force due to the angular acceleration: $m\dot{\boldsymbol{\omega}} \wedge \boldsymbol{r} = -m\omega_0 qx\boldsymbol{k}$.

By (1.1), we get:

$$m \begin{bmatrix} \ddot{x} \\ 0 \\ \ddot{z} \end{bmatrix} = -m \begin{bmatrix} -\omega_0^2(1 - qt)^2 x \\ 2\omega_0(1 - qt)\dot{x} - \omega_0 qx \\ 0 \end{bmatrix} + \begin{bmatrix} -k_2 x \\ R_y \\ R_z - mg \end{bmatrix} + \begin{bmatrix} A\dot{x}(t) \\ 0 \\ 0 \end{bmatrix} \qquad (1.2)$$

namely:

$$\begin{cases} \ddot{x} + A\dot{x}(t) + \left[\dfrac{k_2}{m} - \omega_0^2(1 - qt)^2 \right] x = 0 \\ R_y = 2m\omega_0(1 - qt)\dot{x} - m\omega_0 qx \\ R_z = mg + m\ddot{z} \end{cases} \tag{1.3}$$

Remark 1.1. After adding the second spring, (1.3) shows that as more the origin of the co-mobile frame accelerates with respect to the origin of the fixed one, the more increases the reaction component R_z.

Remark 1.2. The first of (1.3) provides a movement pure equation; the second one gives the y component of constraint reaction after the motion has been solved; the third will allow to evaluate the z component of constraint reaction, after finding the time law $z = z(t)$ of the arm ΩP oscillations.

2 From x-the motion equation to the Hypergeometric Confluent function

Let us integrate the first of (1.3), for shortness represented as:

$$\ddot{x} + A\dot{x} - (at^2 + bt + c)x = 0 \tag{2.1}$$

where $a = q^2\omega_0^2 > 0$, $A > 0$, $b = -2q\omega_0^2 < 0$ and $c = \omega_0^2 - \frac{k_2}{m}$. We state that the general solution of (2.1), putting $\beta = \frac{b^2 - a(A^2 + 4c)}{8a^{3/2}}$ is given by the formula:

$$x(t) = e^{-\frac{at^2 + t(b + \sqrt{a}A)}{2\sqrt{a}}} \left[C_1 \, H_{\beta - \frac{1}{2}} \left(\frac{b + 2at}{2a^{3/4}} \right) + C_2 \, {}_1\mathrm{F}_1 \left(\begin{array}{c} \frac{1}{4} - \frac{\beta}{2} \\ \frac{1}{2} \end{array} \middle| \frac{(b + 2at)^2}{4a^{3/2}} \right) \right] \tag{2.2}$$

where $H_\alpha(t)$ is the Hermite function of nonintegral order α and argument t, while ${}_1\mathrm{F}_1$ is the Kummer function; see for both the Appendix at the end of the paper for some details.

To obtain the analytic solution (2.2) we make twice a variable transformation, the first involving the dependent variable and the second concerning the independent variable, leading to an Hermite differential equation of non integer order for the unknown function $\sigma = \sigma(\tau)$ see formula (A2) in the Appendix. The first transformation of equation (2.1) is obtained putting

$$x(t) = s(t) \exp\left(-\frac{\sqrt{a}At + at^2 + bt}{2\sqrt{a}} \right) \tag{2.3}$$

so that (2.1) is changed in:

$$\ddot{s} - \frac{(2at + b)}{\sqrt{a}}\dot{s} - \frac{\left(4a^{3/2} + aA^2 + 4ac - b^2\right)}{4a}s = 0 \tag{2.4}$$

getting rid of the second degree term in t. Thus (2.4) is of the following type:

$$\ddot{s} - (2m_2 t + m_1)\dot{s} + 2m_0 s = 0. \tag{2.5}$$

where we put:

$$m_2 = \sqrt{a}, \ m_1 = \frac{b}{\sqrt{a}}, \ m_0 = \frac{\left(b^2 - 4a^{3/2} - aA^2 - 4ac\right)}{8a} \tag{2.6}$$

The second step will drive (2.5) into an Hermite equation, see (A2) in the Appendix, by putting

$$t = \frac{\tau}{\sqrt{m_2}} - \frac{m_1}{2m_2} \iff \tau = \sqrt{m_2}t + \frac{m_1}{2\sqrt{m_2}}$$

we obtain the Hermite differential equation, see again (A2) in the Appendix, where we write $\sigma(\tau)$ for $s\left(\frac{\tau}{\sqrt{m_2}} - \frac{m_1}{2m_2} \right)$:

$$\sigma'' - 2\tau\sigma' + 2\frac{m_0}{m_2}\sigma = 0 \tag{2.7}$$

3

Solution (2.2) comes then form formula (A3) combined with (2.3) and (2.6).

The analytical solution of equation (2.1) of our model is then given by (2.2), where:

$$a = \omega_0^2 q^2 > 0, \ b = -2q\omega_0^2 < 0, \ c = \omega_0^2 - \frac{k_2}{m} \lessgtr 0. \tag{2.8}$$

Writing the Lagrange z-motion equation, we get the initial value problem:

$$\begin{cases} \ddot{z} + \dfrac{k_1}{m} z = -g \\ z(0) = z_0 \\ \dot{z}(0) = \dot{z}_0 \end{cases} \tag{2.9}$$

which is solved as:

$$z(t) = C_3 \sin(\overline{\omega}\, t + C_4) - \frac{mg}{k_1} \tag{2.10}$$

with $\overline{\omega} = (k_1/m)^{1/2}$. By the initial conditions $z(0) = z_0$, $\dot{z}(0) = \dot{z}_0$, we get:

$$\begin{cases} C_3 = \sqrt{\left(z_0 + \dfrac{mg}{k_1} \right)^2 + \dfrac{\dot{z}_0^2}{\overline{\omega}^2}} \\ C_4 = \arctan\left(\dfrac{\overline{\omega}(k_1 z_0 + mg)}{\dot{z}_0 k_1} \right) \end{cases}$$

Inserting $z(t)$ given by (2.10) into the third of (1.3), we get the z-component of the reaction:

$$R_z = m[g - C_3 \overline{\omega}^2 \cos(\varpi t + C_4)]. \tag{2.11}$$

The y-component of the reaction requires, see the second of (1.3), x and its time derivative:

$$R_y = 2m\omega_0(1 - qt)\dot{x}(t) - m\omega_0 q x(t). \tag{2.12}$$

The Kummer derivative theorem provides such a derivative, but we omit to relate here its too long expression.

To complete our description, we point out how the polar anomaly θ can be expressed as a time-function. The angular speed is changing during time: the rod $O\Omega$ is first pinning with angular speed ω_0 which, starting from $t = 0$ is affected by a braking torque M_f:

$$\begin{cases} J\dot{\omega} = -M_f \\ \omega(0) = \omega_0 \end{cases} \tag{2.13}$$

So that the angle θ changes in time as

$$\begin{cases} \dfrac{\mathrm{d}\theta}{\mathrm{d}t} = \omega_0(1 - qt) \\ \theta(0) = 0 \end{cases} \tag{2.14}$$

where $q = M_f/J_z\omega_0$ being J_z the inertia axial moment of the shaft.

The reversion of the polar anomaly $\theta = \theta(t)$ provides time as a function of the instantaneous angle, $t = t(\theta)$:

$$\begin{cases} t(\theta) = \dfrac{1}{q}\left(1 - \sqrt{1 - \dfrac{2q\theta}{\omega_0}} \right), \\ 0 \le \theta \le \dfrac{\omega_0}{2q} \end{cases} \tag{2.15}$$

The planar line γ^* is the projection on the fixed plane (e_1, O, e_2), see Figure 3 of the $3 - D$ torse γ. Its equation follows by inserting $t = t(\theta)$ from (2.15) within $x(t)$ which, because of the changed framework, will be renamed as ρ:

$$\begin{cases} \rho = \rho(\theta), \\ 0 \le \theta \le \dfrac{\omega_0}{2q}. \end{cases} \tag{2.16}$$

So that the polar equation of γ^* is obtained.

4

3 A sample problem

The x-problem we faced, is a initial value one with two initial conditions x_0 and v_0, so that the integration constants c_1 and c_2 will depend on: a, b, c, x_0 and v_0. Then the x-solution to (2.2) will be of the kind $x = f(a, b, c; x_0, v_0; t)$. Being the Kummer function unbounded, and in lack of any barrier to x, in carrying out the simulations, it could be possible to see some x behavior not fit with its boundaries.

First of all then we have to state a time span since the forcing transient expires at $t = t_{\lim} = 1/q$. Afterwards, we should subject the function $x(t)$ of (2.2) to a constraint so that x could go never outside the range $(-L, L)$. Notice that x is provided by the (2.2) depending on six variables: then the algorithmic complexity of such a formulation and its low practical usefulness advised us against improving it, so that we restrict here to show how the boundaries could be acted:

$$\begin{cases} -L \leq x(a, b, c; x_0, v_0; t) \leq L \\ 0 \leq t \leq 1/q \end{cases} \tag{3.1}$$

In practice, we assumed as a sample problem, the following physical data, stopping the computation whenever should $x(t)$ go out its boundaries.

$L = 1m;$ $\qquad\qquad k_1 = 10Nm^{-1};$ $\qquad\qquad q = s^{-1}$, variable;

$H = 3m;$ $\qquad\qquad k_2 = Nm^{-1}$, variable;

$m = 1kg;$ $\qquad\qquad \omega_0 = 3\mathrm{rad}s^{-1};$

where the k_2 values (Nm^{-1}) for transients I, II, III, IV, V respectively, are: 10; 8; 30; 8, ... The q values (s^{-1}) for transients I, II, III, IV respectively, are: 1/10, 1/10, -1/10,-1/10. We carried out five transients.

Notice that $c = \omega_0^2 - \frac{k_2}{m}$ has dimension of a square of a frequency and sets up a comparison on the resulting bead motion between the centrifugal outside cause ω_0 and the spring opposition measured by $\frac{k_2}{m}$. Therefore the most studied occurrence $c < 0$ (transients I, II, III, V) means that the elastic influence is prevailing on the rotational starting speed.

3.1 I transient: ω shutdown with major elastic force influence

By formulae (2.8) we see that both a and b signs do not depend on k_2, while the mix of values of m, k_2, ω_0 decides that of $c = \omega_0^2 - \frac{k_2}{m}$. Let be $\frac{k_2}{m} > \omega_0^2$: then the elastic spring force will be, at the beginning, of greater effect than the centrifugal one, so that x-oscillations will occur and will expire with the angular speed, see Figure 2
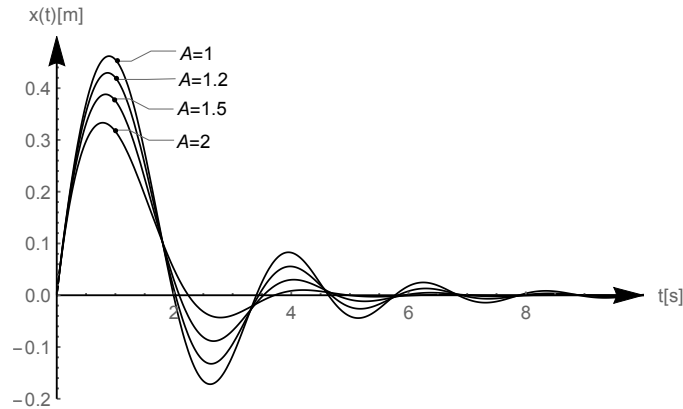

Figure 2: I transient: ω shutdown with prevailing elastic force ($c < 0$): (x, t)-oscillations under four different A drag values.

We can also compute by the second of (1.3) the oscillations of reaction R_y which is affecting the bead: see Figure 4. Putting $t = t(\theta)$ within $x(t)$, we get the polar plot, to be read counterclockwise, of the curve γ^* projection of the torse γ on the fixed plane $(\boldsymbol{e_1}, O, \boldsymbol{e_2})$, see Figure 1 and Figure 3.
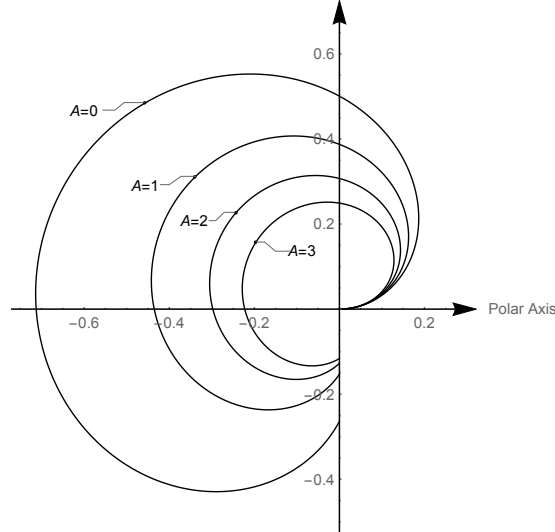
Figure 3: ω shutdown with prevailing elastic influence: polar plot $\rho = \rho(\theta)$ of the $\gamma^\star$ projection of the bead's torse. Four different A-drag values.

3.2 II transient: ω shutdown with minor elastic influence: oscillations.

The simulations with smaller k_2 values produced not-oscillatory behaviors, here omitted for shortness. Increasing k_2 values, the effect of the elastic forces is not too weak, so that reactions will oscillate. We provide only the plot of R_y versus t, Figure 4
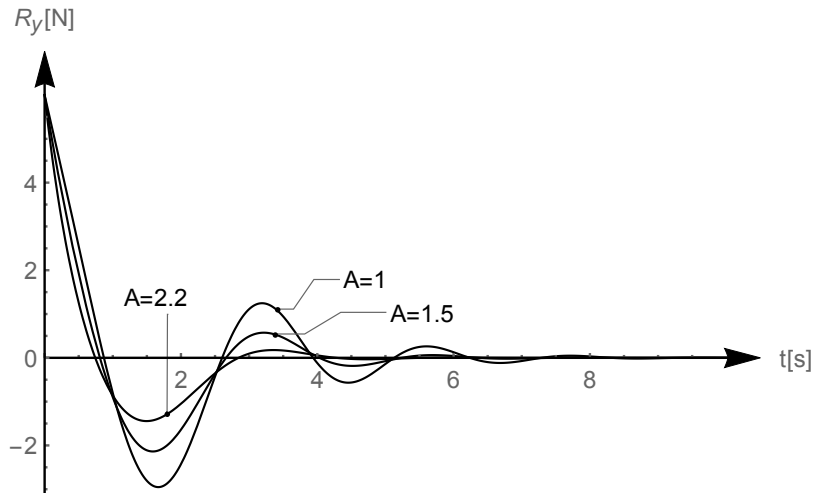

Figure 4: II transient: ω shutdown with prevailing elastic force, $c < 0 : (R_y, t)$-oscillations under different A drag values.

3.3 III transient: ω increasing with major elastic influence

By (2.8) we see that the ω increase, namely $q < 0$, impacts on the sign of b, and then on the exponential factor responsible of the drop of x, according to (2.2). We see the major elastic influence, $c < 0$, succeeds in producing decaying oscillations again, see Figure 5, but at the end the (x, t) plot will blow-up in any case.
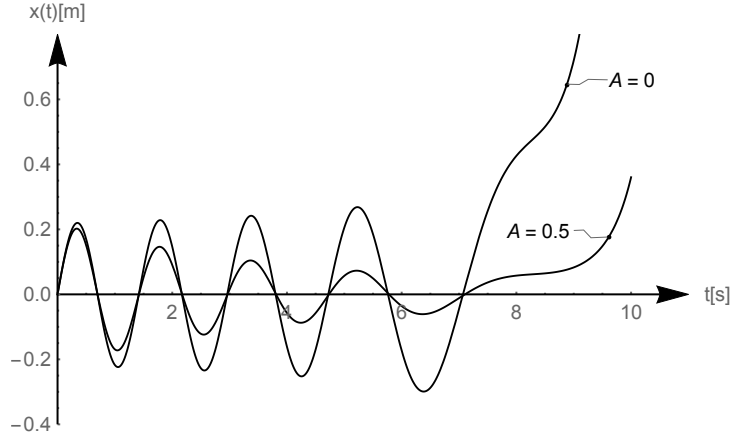
Figure 5: III transient: ω increasing with major elastic influence, $c < 0$: bead's (x, t)-oscillatory first course and final blow-up. Different A drag values.

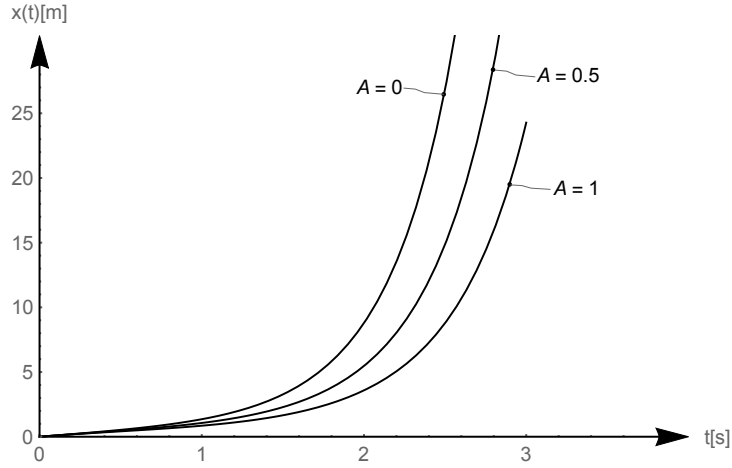

Figure 6: IV transient: ω increasing with not-oscillatory bead's (x, t)-plot. Different A drag values.

3.4   IV transient: ω increasing with minor elastic influence, non-oscillatory bead's x-behaviour

Here, see Figure 6, we can see how the double event of the ω growth and the minor elastic influence, $c > 0$, will produce an x-monotonic path whose plot has been cut-off about the third second due to its blowing-up.

We know that oscillations occur when in a system's structure the elastic features are the prevailing ones. Figure 5 shows how this happens for the first times when ω is not yet so large. Next, when the rotational effects will prevail, the vibrations do cease at all and the motions tend to instability with or without damping which can affect only the blow-up rate.

Remark 3.1. Specially for those transients where ω, and then the centrifugal force, grows, the knowledge of the time law of the transverse R_y of the rod-blade on the block, will provide, by reaction, the loads acted by the block on the blade itself. In such a way, a comparative check on the ω range, will define the dynamic safety levels for the rod during the start-up transients.

3.5   V transient

Here we are analyzing a transient where we assume the angular speed to be a constant, $q = 0$, $\omega(t) = \omega_0$, and with $c < 0$ as before, namely the elastic forcing keeps its control over the centrifugal one. We can then expect pure x-oscillations whose expiring time is ruled by the damping A amount. The motion equation collapses in a constant coefficients one.
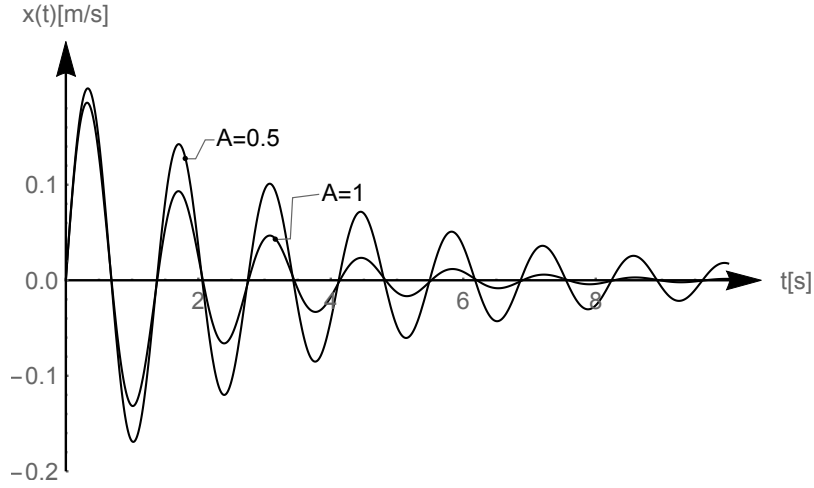
7

Figure 7: V transient: ω constant with mayor elastic influence, $c < 0$: damped oscillations.

3.6 Summary

The main features of all transients ruled by the homogeneous Weber equation (2.1) are summarized below

Transient N.	$\omega(t)$ behavior	$c = \omega_0 - \frac{k}{m^2}$	Main computed effects	Figure N.
I	shutdown	$c_I < 0$	Clear x oscillations, different dampings	Figure 2
			The head's curve projections are spiralizing	Figure 3
II	shutdown	$c_{II} < c_I < 0$	Oscillations of constraint reaction R_y	Figure 4
III	increasing	$c_{III} < 0$	Initially x oscillates but at end blows up	Figure 5
IV	increasing	$c_{IV} > 0$	The x monotonic increase plot	Figure 6
V	constant $= \omega_0$	$c_V < 0$	Some x oscillations without blow-up, all expiring sooner or later according to the damping A	Figure 7

4 The forced case adding dry friction too

By adding into the system an outside forcing μ which models both effects of a blade inclination and a dry friction contact, the previous motion equation becomes inhomogeneous:

$$\begin{cases} \ddot{x}(t) + A\dot{x}(t) - (at^2 + bt + c)x(t) = \mu \\ x(0) = 0 \\ \dot{x}(0) = 1, \end{cases} \tag{4.1}$$

with $\mu \in \mathbb{R}$ is homogeneous to an acceleration. Applying the Lagrange variation of parameters method[2], the particular integral will be provided by:

$$\overline{x}(t) = c_1(t)x_1(t) + c_2(t)x_2(t) \tag{4.2}$$

being $c_1(t)$ and $c_2(t)$ given by:

$$c_1(t) = -\mu \int \frac{x_2(t)}{\dot{x}_2(t)x_1(t) - x_2(t)\dot{x}_1(t)} \mathrm{d}t, \tag{4.3}$$

---

[2]Between 1778 and 1783, Lagrange developed his method in papers concerning the variations in planetary motions and in another series of memoirs on computing the orbit of a comet from three observations. During 1808-1810, he gave to the method its final form in a series of papers among which we shall quote [11] which is available at Gallica web site

and:

$$c_2(t) = \mu \int \frac{x_1(t)}{\dot{x}_2(t)x_1(t) - x_2(t)\dot{x}_1(t)} \mathrm{d}t. \tag{4.4}$$

Mind that $x_1(t)$ and $x_2(t)$ are two linearly independent integrals of the homogeneous equation which can be read on (2.2):

$$x_1(t) = e^{-\frac{at^2 + t(b+\sqrt{a}A)}{2\sqrt{a}}} H_{\beta - \frac{1}{2}}\left(\frac{b+2at}{2a^{3/4}}\right) \tag{4.5}$$

and

$$x_2(t) = e^{-\frac{at^2 + t(b+\sqrt{a}A)}{2\sqrt{a}}} {}_1F_1\left(\begin{array}{c} \frac{1}{4} - \frac{\beta}{2} \\ \frac{1}{2} \end{array}\middle| \frac{(b+2at)^2}{4a^{3/2}}\right). \tag{4.6}$$

In order to avoid a fully numerical solution we decided an approach by which, even if resorting to definite numerical integrations, we are however allowed to keep the control of the solution's functional structure. Both integrals (4.3), (4.4) cannot be computed analytically: nevertheless we can resort to a series expansion of the integrand. Let us see first the function $c_1(t)$.

Formula (4.3) is of kind:

$$c_1(t) = -\frac{8a^2\mu}{4a^{3/2} - b^2 + a(A^2 + 4c)} \int f(t)\mathrm{d}t, \tag{4.7}$$

where:

$$f(t) = \frac{e^{\frac{at^2 + t(b+\sqrt{a}A)}{2\sqrt{a}}}}{u_1(t) + u_2(t)} {}_1F_1\left(\begin{array}{c} \frac{1}{4} - \frac{\beta}{2} \\ \frac{1}{2} \end{array}\middle| \frac{(b+2at)^2}{4a^{3/2}}\right) \tag{4.8}$$

being in it:

$$u_1(t) = 2a^{3/4} H_{\beta - \frac{3}{2}}\left(\frac{b+2at}{2a^{3/4}}\right) {}_1F_1\left(\begin{array}{c} \frac{1}{4} - \frac{\beta}{2} \\ \frac{1}{2} \end{array}\middle| \frac{(b+2at)^2}{4a^{3/2}}\right) \tag{4.9}$$

and:

$$u_2(t) = (b+2at) H_{\beta - \frac{1}{2}}\left(\frac{b+2at}{2a^{3/4}}\right) {}_1F_1\left(\begin{array}{c} \frac{5}{4} - \frac{\beta}{2} \\ \frac{3}{2} \end{array}\middle| \frac{(b+2at)^2}{4a^{3/2}}\right). \tag{4.10}$$

We now go on by showing how $c_1(t)$ can be evaluated by means of a sample problem. Let us choose for instance the case $A = 1$, $a = 9/100$, $b = -9/5$, $c = -1$, $\mu = $ undefined. By (4.7) we see the solution $x(t)$ is by the physical problem defined for $t \in [0, 1/q]$; so that, with $1/q = 10$, the physical range representation of solution is $t \in [0, 10]$. We could try to model our specific $f(t)$, say $\hat{f}(t)$, in such a range by means of a MacLaurin polynomial $T_{200}(t)$ holding 200 terms: Figure 8 shows
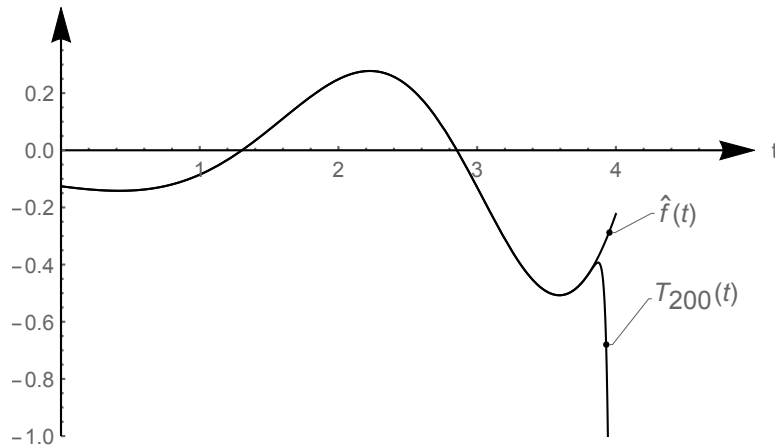

Figure 8: Sketch of both curves $\hat{f}(t)$ and $T_{200}(t)$. The ordinate computed values have been multiplied by 10^{14}.

that before four seconds the approximation fails and the dissimilarity takes such a shape due to

9

the very high powers involved in Taylor polynomial. We then try for $\hat{f}(t)$ a Fourier-Bessel series expansion, in terms of the Bessel function of order zero J_0, see [12]:

$$\hat{f}(t) = \sum_{k=1}^{+\infty} B_k J_0\left(\frac{\alpha_k}{\bar{t}}t\right), \tag{4.11}$$

where denoting as usual J_0 and J_1 the first kind Bessel functions of order 0 and 1 respectively. The B_k coefficients can be computed as:

$$B_k = \frac{2}{\bar{t}^2 J_1^2(\alpha_k)} \int_0^{\bar{t}} t\hat{f}(t)J_0\left(\frac{\alpha_k}{\bar{t}}t\right)dt \tag{4.12}$$

to which the condition to be added is:

$$J_0(\alpha_k\bar{t}) = 0. \tag{4.13}$$

In previous lines $\bar{t}$ is the root of function $\hat{f}(t)$ and α_k is the sequence of roots of J_0 provided by the formula of McMahon [13]. We did use the function J_0 because it shall be $\hat{f}(0) \neq 0$. Such a representation fits perfectly $\hat{f}(t)$ and 200 terms provide (with $A \neq 0$) a satisfactory convergence (but with $A = 0$ only 30 terms are enough). We pass to integrate $\hat{f}(t)$ as in (4.7). We choose to express the integral of J_0 in terms of generalized hypergeometric function $_1F_2$

$$\int J_0(\gamma t)dt = {}_1F_2\left(\begin{array}{c} \frac{1}{2} \\ 1, \frac{3}{2} \end{array} \middle| -\frac{\gamma^2}{4}t^2\right) \tag{4.14}$$

Such a relationship can be found in [14], page 44; inserted into the $c_1(t)$ formula, it provides:

$$c_1(t) = -\frac{8a^2\mu}{4a^{3/2} - b^2 + a(A^2 + 4c)} t \sum_{k=1}^{+\infty} B_k \, {}_1F_2\left(\begin{array}{c} \frac{1}{2} \\ 1, \frac{3}{2} \end{array} \middle| -\frac{\alpha_k^2}{4\bar{t}^2}t^2\right). \tag{4.15}$$

So the series truncation can be done after the integration and not before, so that the approximation will result of better quality. Let us now compute the value of $\bar{t}$, namely the root of function $\hat{f}(t)$ subsequent to the end ($t = 10$) of the physical range of $x(t)$. We find: $\bar{t} = 10.5031$. We shall then expect a $\hat{f}(t)$ representation converging with a relatively small number of terms. And in fact with 120 terms of the expansion (4.11) of $\hat{f}(t)$ we get a satisfactory fit for $t \in [0, 10]$.

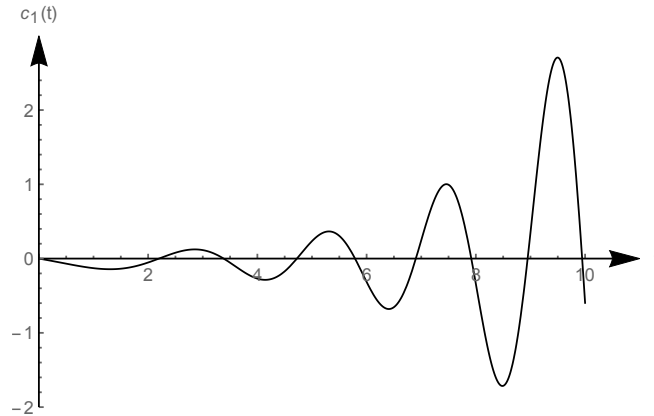Assuming $\mu = 1$, by (4.15) we get $c_1(t)$ whose plot is shown:

Figure 9: Plot of function $c_1(t)$ to be put in (4.2): the ordinate computed values have been multiplied by 10^{14}.

The same can be done in order to $c_2(t)$. The particular integral has been evaluated for $\mu = 1$, but, due to formulae (4.3) and (4.4), its amplitude is just μ. The general integral is got adding it to that of the homogeneous equation. We provide such a $\mu = 1$ forced case description through some curves for different A values. Notice that for drag values $A > 2$ no oscillatory behavior occurs any more and the overdamping takes place.
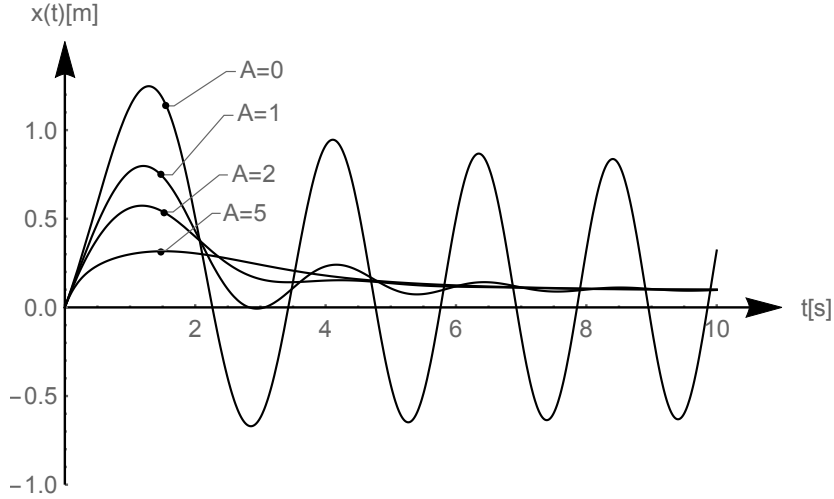
Figure 10: The forced case: damped oscillations, different A values and under dry friction, $\mu = 1$.

5 Conclusions

The main features of our viscous and non inertial oscillator are included in (1.3) where the $x-$equation, a Weber one, solved by means of the Hermite and Kummer functions, see (2.2). Our model has been analyzed carrying out five sample transients. In all cases the effects of the ω outside law, starting at $t = 0$, are stopped at $t = 10s$. Figure 2 describes the x-oscillations whenever the angular speed ω is falling down: some viscous drag values have been considered in presence of a meaningful elastic force. The same problem has then been seen differently and we provide a polar plot of the bead torse's projection. The second transient shows the oscillating behavior of the constraint reaction R_y under major elastic effects. The third case takes into account a linear ω growth: Figure 5 shows the oscillatory amplitudes' different increase according to different drag A values. The fourth case displays a nonoscillatory behavior. The last one assumes the angular speed to be kept constant. Four of the above cases assume the rotating speed changing in time, different viscous drags, but no dry friction, namely $\mu = 0$. Taking into account the dry friction on the bead too, the ODE keeps its linearity but looses its homogeneity. Figure 10 plots a set of damped oscillations with different A values and forced by dry friction $\mu = 1$.

Appendix

The first hypergeometric series appeared in a Wallis's book [15]:

$$
{}_2\mathrm{F}_1 \left(\begin{array}{c} a; b \\ c \end{array} \middle| x \right) = \sum_{n=0}^{\infty} \frac{(a)_n \, (b)_n}{(c)_n} \frac{x^n}{n!},
$$

for $|x| < 1$ and complex parameters a, b, c being $(a)_n$, $(b)_n$, $(c)_n$ Pochhammer symbols, for instance:

$$
(a)_n = \frac{\Gamma(a + n)}{\Gamma(a)}
$$

being Γ the Euler factorial functions. Function ${}_2\mathrm{F}_1$ solves the linear second order Gauss differential equation for the unknown $u(x)$:

$$
x(1 - x)\, u'' + [c - (a + b + 1)\, x]\, u' - ab\, u = 0 \tag{A1}
$$

Furthermore, many functions have been introduced in 19th century either for generalizing it to multiple variables or taking the special way of *confluence*. This is the case of the Kummer CHF, defined by the absolutely convergent infinite power series:

$$
{}_1\mathrm{F}_1 \left(\begin{array}{c} a \\ c \end{array} \middle| x \right) = \sum_{n=0}^{\infty} \frac{(a)_n}{(c)_n} \frac{x^n}{n!}.
$$

11

It is analytic, regular at zero entire single-valued transcendental function of all a, c, x, (real or complex) except $c = 0, -1, -2, -3, \ldots$, for which it has simple poles. The above series is a solution of the Kummer ordinary differential equation in $y(x)$:

$$xy'' + (c - x)y' - ay = 0, \qquad \text{(K)}$$

A detailed but compact outline of CHF integral representation, asymptotic and formulæ of various functions through it, can be found in [18].

The French mathematician C. Hermite (1822-1901) considered the second order differential equation in $v(z)$:

$$v'' - 2zv' + 2\nu v = 0, \qquad \text{(A2)}$$

The general solution of (A2) is

$$v(z) = c_1 H_\nu(z) + c_2 \, {}_1\mathrm{F}_1 \left(\begin{array}{c} -\frac{\nu}{2} \\ \frac{1}{2} \end{array} \middle| z^2 \right) \qquad \text{(A3)}$$

where $H_\nu(z)$ is the *Hermite function* of degree ν of the real variable z. If ν is an integer, $H_\nu(z)$ reduces to the *Hermite polynomials* of degree ν. Such polynomials are a certain subclass of the so called orthogonal polynomials and are met solving the simple harmonic oscillator of quantum mechanics. On the contrary, if ν is not an integer, as in our case, the Hermite function is a linear combination of Kummer functions, namely:

$$H_\nu(z) = \sqrt{\pi}\, 2^\nu \left(\frac{1}{\Gamma\left(\frac{1-\nu}{2}\right)} \, {}_1\mathrm{F}_1 \left(\begin{array}{c} -\frac{\nu}{2} \\ \frac{1}{2} \end{array} \middle| z^2 \right) - \frac{1}{\Gamma\left(-\frac{\nu}{2}\right)} 2z \, {}_1\mathrm{F}_1 \left(\begin{array}{c} \frac{1-\nu}{2} \\ \frac{3}{2} \end{array} \middle| z^2 \right) \right).$$

Finally in the paper appeared a ${}_1\mathrm{F}_2$ function, whose power series is

$$ {}_1\mathrm{F}_2 \left(\begin{array}{c} a \\ b_1,\, b_2 \end{array} \middle| x \right) = \sum_{n=0}^\infty \frac{(a)_n}{(b_1)_n (b_2)_n} \frac{x^n}{n!} \qquad \text{(A3)}$$

which converges for any $x \in \mathbb{C}$. Even if this function we did not appear in any differential in the paper, we point out that it is solution of the third order differential equation in the unknown $w(z)$

$$z^2 w^{(3)} + (b_1 + b_2 + 1)\, zw'' + (b_1 b_2 - z)\, w' - a_1 w = 0.$$

Acknowledgements

References

[1] E. E. Kummer, De integralibus quibusdam definitis et seriebus infinitis, Journal für die reine und angewandte Mathematik 17 (1837) 228–242.

[2] G. Mingari Scarpello, D. Ritelli, Elliptic integral solutions of spatial elastica of a thin straight rod bent under concentrated terminal forces, Meccanica 5 (41) (2006) 519–527.

[3] G. Mingari Scarpello, D. Ritelli, Exact solutions of nonlinear equation of rod deflections involving the Lauricella hypergeometric functions, Int. J. Math. Math. Sci. (2011) Art. ID 838924.

[4] G. Mingari Scarpello, D. Ritelli, Closed form integration of a hyperelliptic, odd powers, undamped oscillator., Meccanica 47 (4) (2012) 857–862.

[5] H. Lauwerier, The use of confluent hypergeometric functions in mathematical physics and the solution of an eigenvalue problem, Appl. Sci. Res. A2 (1950) 184–204.

[6] J. Seaborn, Hypergeometric functions and their applications, Springer Verlag, 1982.

[7] L. Slater, Generalized hypergeometric functions, Cambridge University Press, 1966.

[8] F. Tricomi, Funzioni ipergeometriche confluenti, Cremonese, 1954.

[9] G. Georgiev, M. Grosse, The Kummer confluent hypergeometric function and some of its applications in the theory of azimuthally magnetized circular ferrite waveguides, Journal of telecommunications and information technology 3 (2005) 112–128.

[10] D. Nagar, R. Moran, A. Gupta, Properties and applications of extended hypergeometric functions, Ingenierìa y Ciencia 10 (19) (2014) 11–31.

[11] J. Lagrange, Sur la théorie générale de la variation des constantes arbitraires dans tous les problémes de la méchanique, Mémoires de la première classe de l'Institut de France (1809) 771–805.

[12] G. Watson, A treatise in the theory of Bessel functions, Cambridge University Press, 1944.

[13] J. McMahon, On the roots of the Bessel and certain related functions, The Annals of Mathematics 9 (1/6) (1894) 23–30.

[14] Y. L. Luke, Integrals of Bessel functions, McGraw-Hill, 1962.

[15] J. Wallis, Arithmetica infinitorum, Robinson, 1656.

[16] J. Dutka, The early history of the hypergeometric function, Archive for History of Exact Sciences 31 (1) (1984) 15–34.

[17] A. M. Legendre, Exercices de calcul intégral, Courcier, 1811.

[18] N. Lebedev, Special Functions & their applications, Dover, 1972.